Electronic Supplementary Information

Self-supported tripod-like nickel phosphide nanowire arrays for hydrogen evolution

Yue Wang,[a,b] Lina Liu,[a] Xiao Zhang,[a] Feng Yan,[a] Chunling Zhu,[b] and Yujin Chen [a*]*

a Key Laboratory of In-Fiber Integrated Optics, Ministry of Education, and College of Science, Harbin Engineering University, Harbin 150001, China.

b College of Material Science and Chemical Engineering, Harbin Engineering University, Harbin 150001, China.

*Corresponding authors.

E-mail addresses: chenyujin@hrbeu.edu.cn, zhuchunling@hrbeu.edu.cn

EXPERIMENTAL SECTION

1. Materials and Methods.

Nickel acetate, ammonium molybdate, potassium hydroxide, concentrated hydrochloric acid, and ethanol were purchased from Tianjin Guangfu Fine Chemical Research Institute (China). Sodium hypophosphite was purchased from Tianjin Tianli Chemical Reagent Co., Ltd. Ni foam was purchased from Kunshan Yiersheng International Trade Co. Ltd (Kunshan, China). Commerical IrO_2 and 20 wt% Pt/C catalysts were purchased from Macklin Biochemical Co., Ltd (Shanghai, China). All chemicals were used as received and all aqueous solutions were prepared using ultrapure water (>18.2 MΩ).

2. Synthesis of Ni_xP

The $NiMoO_4 \cdot xH_2O$ nanowires were synthesized on NF according to the previously reported method.[S1] The $Ni(OH)_2$-NiOOH/NF tripod-like nanostructure was made by leaching the Mo from surface of $NiMoO_4 \cdot xH_2O$ nanowires through electrochemical oxidation at 1.59 V versus reversible hydrogen electrode (RHE) for about 20 min in 1.0 M KOH. The Ni_xP catalyst was synthesized by one-step phosphorization. The precursor of NaH_2PO_2 powder was placed at the upstream during the phosphorization, and a small piece of $Ni(OH)_2$-NiOOH on Ni foam (~ 2.2 cm×2.6 cm) was placed at the middle of tube furnace at a Ar gas flow. The pyrolysis treatment performed at 300, 400, and 500 °C for 1 h were denoted as Ni_xP-300, Ni_xP-400 and Ni_xP-500, respectively.

3. Synthesis of $NiMoO_4$-P

To prepare $NiMoO_4$-P NWs, the $NiMoO_4$/NF and NaH_2PO_2 were put at two separate positions in the porcelain boat with NaH_2PO_2 of 500 mg at the upstream side of the tube furnace. And then heat treated at 600 °C for 2 h at the Ar atmosphere.

4. Synthesis of $Ni(OH)_2$-P/NF

The $Ni(OH)_2$ nanosheets were prepared by one step hydrothermal reaction according to a previous report.[S2] Then the synthesis procedure of $Ni(OH)_2$-P is similar to that of Ni_xP-400, expect that replaced $Ni(OH)_2$-NiOOH/NF with $Ni(OH)_2$/NF.

5. Synthesis of NF-P

For comparison, the NF-P was directly synthesized according to the method of the Ni_xP-400, expect that replaced $Ni(OH)_2$-NiOOH/NF with the bare Ni foam.

6. Synthesis of $FeNi(OH)_x$/NF

The $FeNi(OH)_x$/NF was synthesized on NF according to the method previously reported by our group.[S3]

7. Structure characterization

The powder X-ray diffraction (XRD) patterns were recorded on a Panalytical X-pert diffractometer with Cu Kα radiation (λ=1.5418 Å). The morphology and composition of the electrocatalysts were analyzed by scanning electron microscopy (SEM) (Hitachi SU70), and transmission electron microscopy (TEM) (FEI Tecnai-F20 transmission electron microscope). XPS analyses were acquired by using X-ray Photoelectron Spectroscopy (XPS, Themofisher Scienticfic Company) with Al Kα radiation.

8. Electrochemical Measurements

The HER activitiy was performed with a CHI760E electrochemical workstaion in the 1.0 M KOH aqueous electrolyte with a standard three-electrode electrochemical cell. It is important to mention that the 3D self-supported Ni_xP and $NiMoO_4$-P catalysts, without any binder or conductive agent, were directly used as working electrodes. The area of the working electrodes immersed into the electrolyte was controlled to be 1 cm^2. A saturated Ag/AgCl electrode was used as the reference electrode and a graphite rod was used as the counter electrode. 20wt% Pt/C and IrO_2 electrodes were prepared as follows: The catalyst powder was dispersed in N-methyl-2-pyrrolidone solvent containing 7.5 wt% PVDF under constant stirring. The weight ratio of the catalyst to PVDF was 8:1. Then the mixture was coated onto a piece of Ni foam. The amount of the catalysts on the Ni foam was about 1.5 mg cm^{-2}. All the measurements were carried out at ambient temperature. The HER activities of the self-supported electrodes were evaluated by comparing the polarization curves obtained using linear sweep voltammetry (LSV) at a scan rate of 5 mV s^{-1}. Tafel analyses were carried out according to the following Tafel equation: $\eta = a + b \log|j|$, where a is a constant, b is the Tafel slope and j is the current density. Doule-layer capacitance (C_{dl}) data were collected via the cyclic voltammetry curves measured, the potentials were between 0.2 and 0.3 V vs. RHE, and the scanning rates were from 100 to 300 mV s^{-1}. Electrochemical impedance spectroscopy (EIS) measurements were performed by

applying an AC voltage with 5 mV amplitude in a frequency range from 0.01 Hz to 100 kHz. The chronopotentiometric measurements were used to assess the long-term stability of the electrocatalysts. All potentials measured were calibrated to reversible hydrogen electrode (RHE) using the following equation: $E_{RHE} = E^{0}_{Ag/AgCl} + 0.21 + 0.059 \times pH$. All LSV curves reported in this work are corrected by *iR* loss according to the following formula: $E_{compensated} = E_{measured} - iR$, where $E_{compensated}$ is the compensated potential, $E_{measured}$ the measured potentials and *R* the equivalent series resistance that was determined by the current interrupt technique.

The electrochemical performance of the overall water splitting system assembled with $FeNi(OH)_x$/NF as anode and Ni_xP-400 as cathode was evaluated in 1.0 M KOH through LSV at a scan rate of 5 mV s^{-1}. For comparison, the electrochemical performance of the electrolyzer assembled with Pt/C and IrO_2 was also measured under the same conditions.

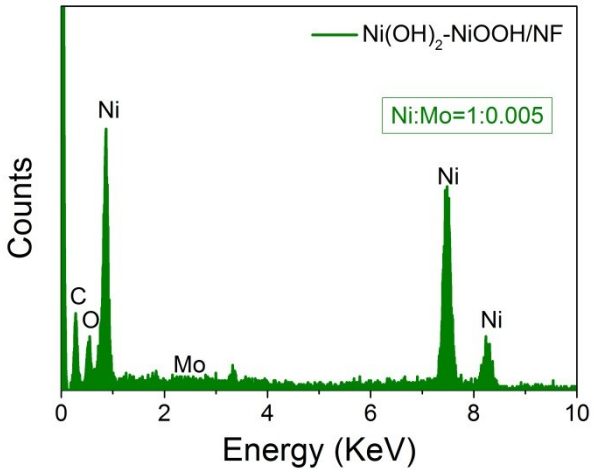

Fig. S1 SEM-EDS spectrum of $Ni(OH)_2$-NiOOH/NF.

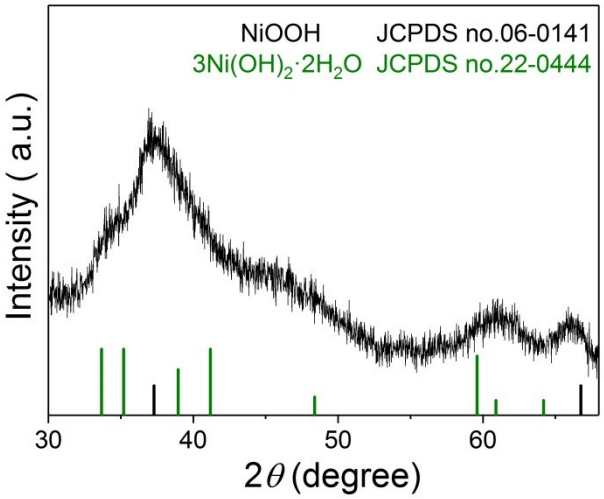

Fig. S2 XRD pattern of $Ni(OH)_2$-NiOOH NWs.

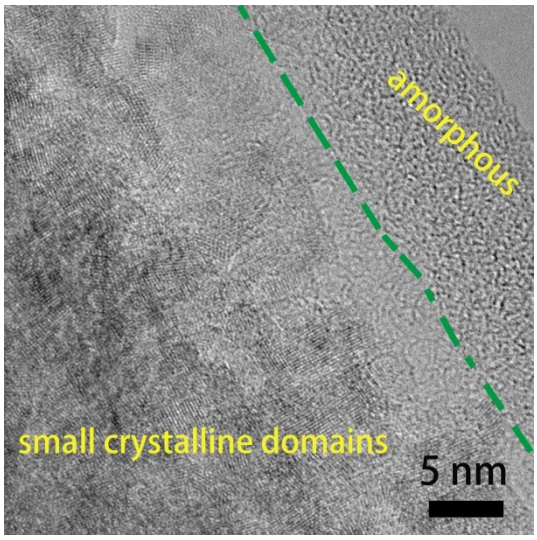

Fig. S3 HRTEM image of $Ni(OH)_2$-NiOOH NW.

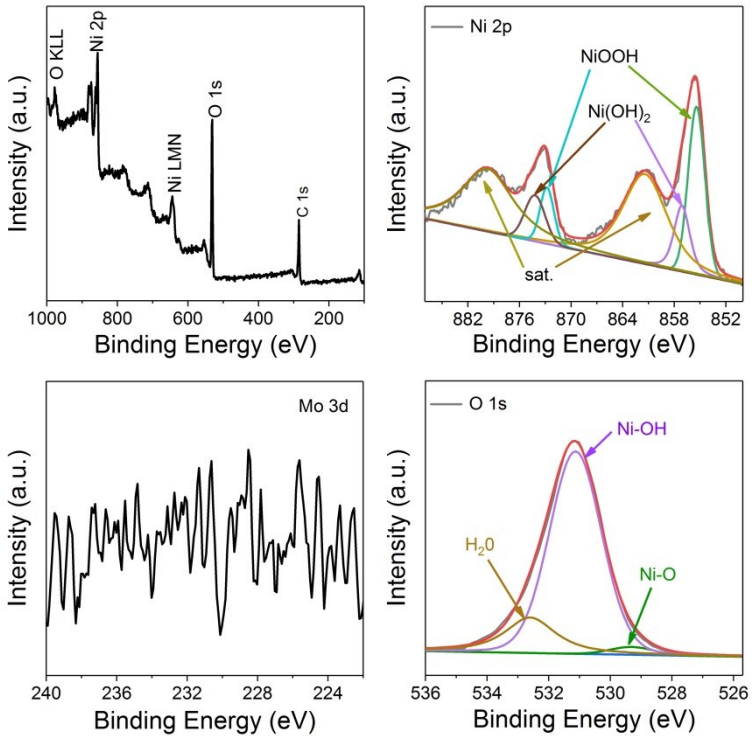

Fig. S4 XPS spectra of a) survey scan, b) Ni 2p, c) Mo 3d, and d) O 1s for the $Ni(OH)_2$-NiOOH NWs.

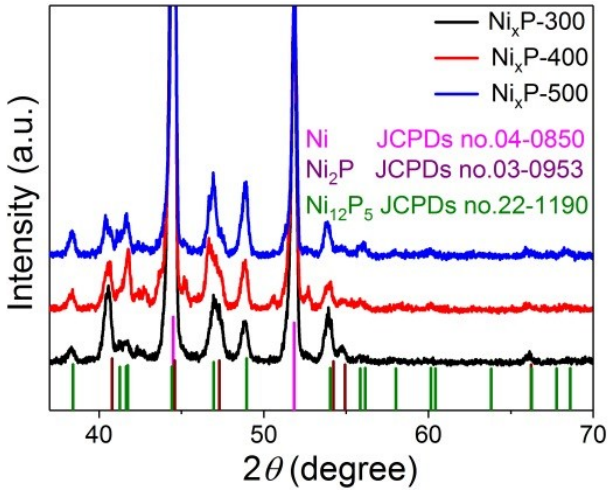

Fig. S5 XRD patterns of Ni_xP-300/NF, Ni_xP-400/NF, and Ni_xP-500/NF.

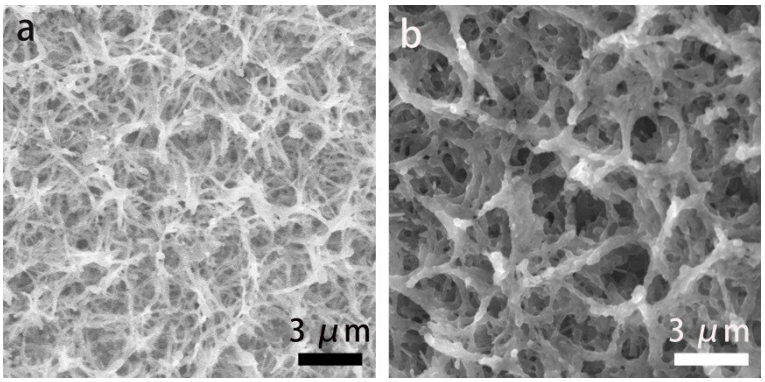

Fig. S6 SEM images of a) Ni_xP-300/NF, and b) Ni_xP-500/NF.

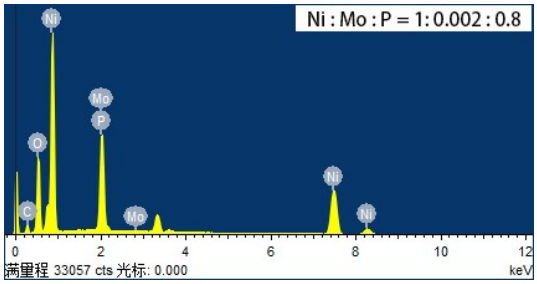

Fig. S7 SEM-EDS spectrum of Ni_xP/NF-400.

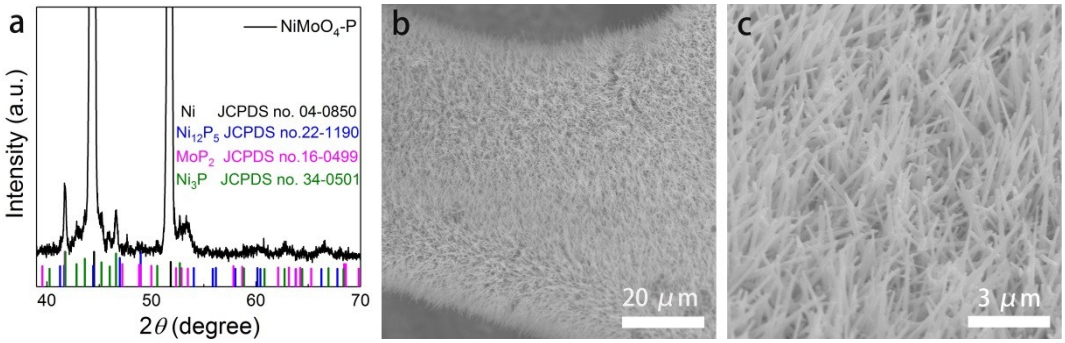

Fig. S8 a) XRD pattern of $NiMoO_4$-P/NF. b, c) SEM images of $NiMoO_4$-P/NF.

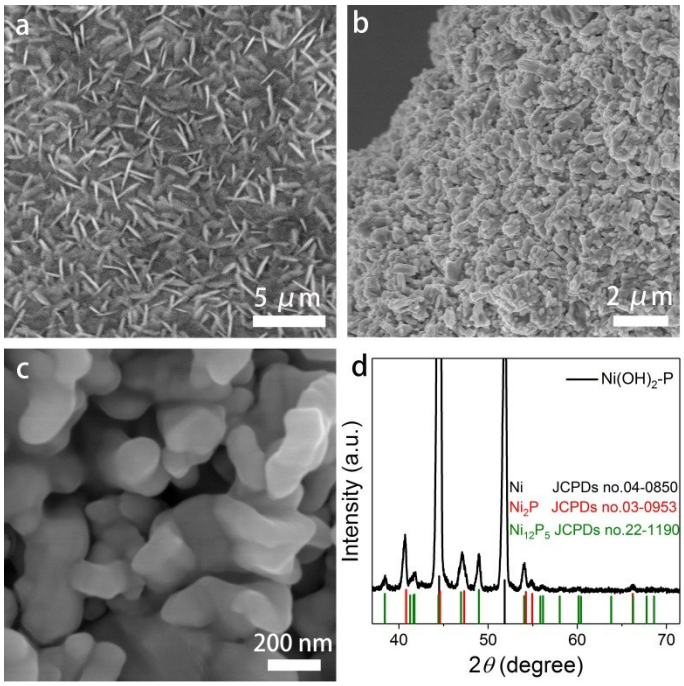

Fig. S9 a) SEM image of $Ni(OH)_2$/NF. b, c) SEM images of the $Ni(OH)_2$-P, and d) XRD pattern of $Ni(OH)_2$-P.

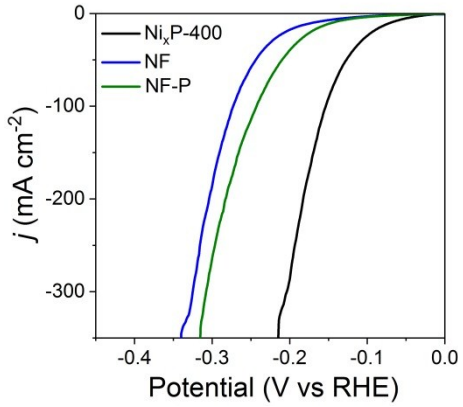

Fig. S10 LSVs of Ni_xP-400 NWs, bare NF and NF-P catalysts.

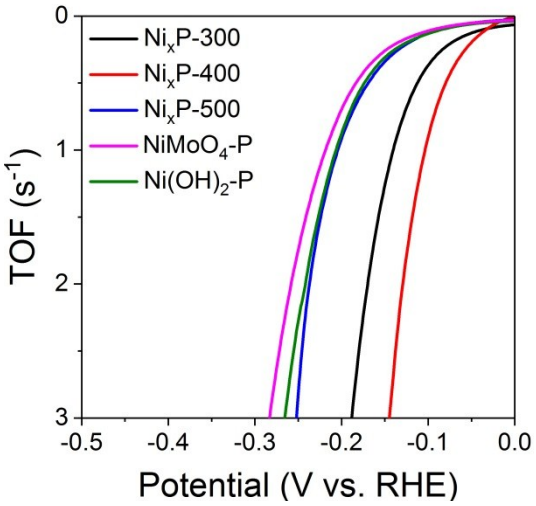

Fig. S11 Calculated turnover frequencies of the Ni_xP-300, Ni_xP-400, Ni_xP-500, $NiMoO_4$-P and $Ni(OH)_2$-P electrodes in 1.0 M KOH for HER process.

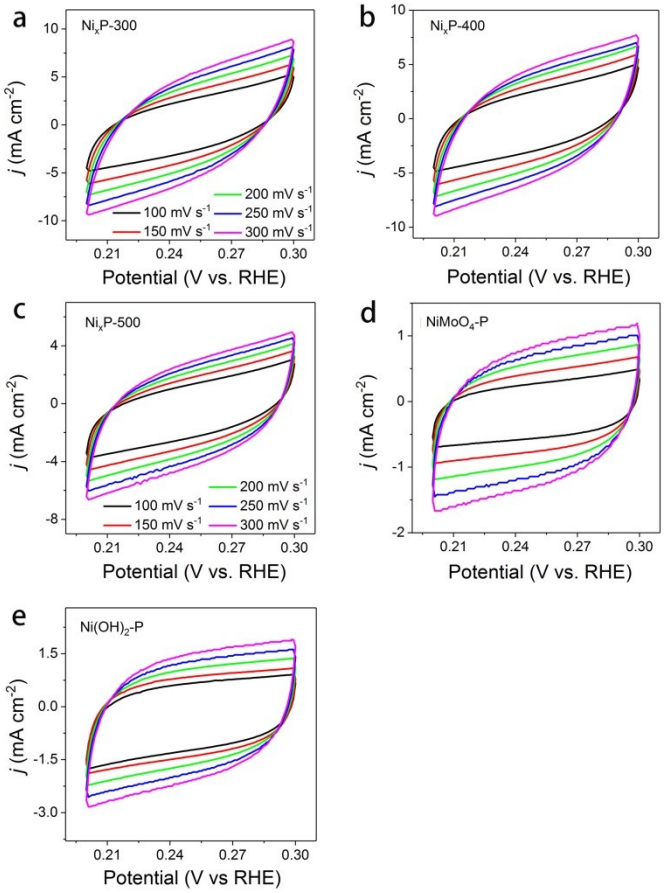

Fig. S12 CV curves for a) Ni_xP-300, b) Ni_xP-400, c) Ni_xP-500, d) $NiMoO_4$-P and e) $Ni(OH)_2$-P electrodes in the region of 0.2 and 0.3 V vs. RHE at different scan rates (100, 150, 200, 250 and 300 mV s^{-1}).

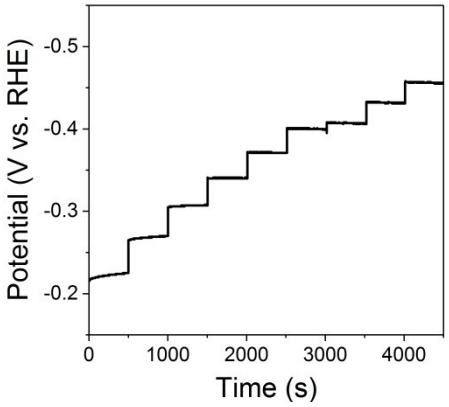

Fig. S13 The multi-step chronopotentiometric curve of the Ni_xP-400 electrode towards the HER without *iR* corrections.

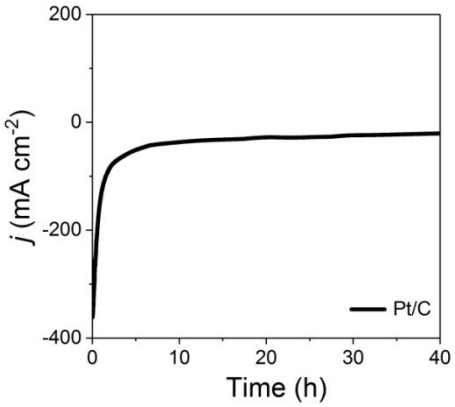

Fig. S14 The time-dependent current density curve of Pt/C for 40 h.

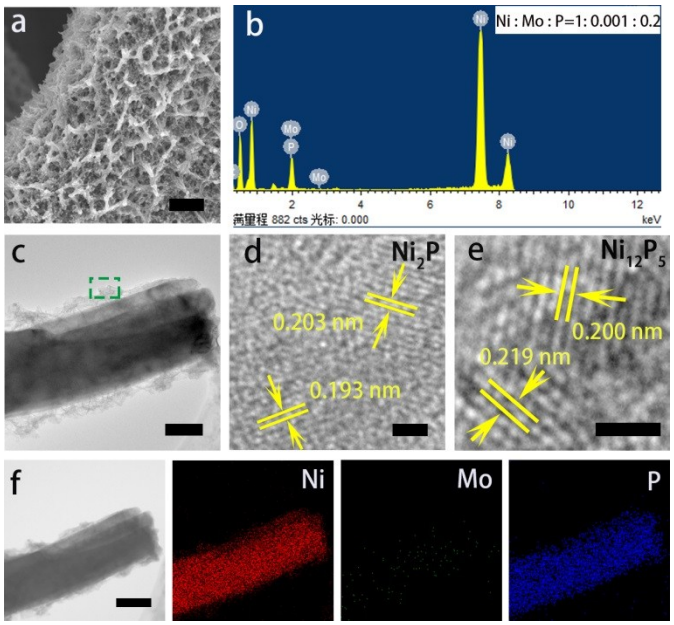

Fig. S15 a) SEM image, b) SEM-EDX spectrum of the Ni_xP-400/NF after HER stability test. The scale bars in a): 5 µm. c) TEM image, d, e) HRTEM images from the selected part of the c), and f) STEM image and corresponding EDX elemental mapping images of Ni_xP-400 NWs after HER stability test. The scale bars in c): 50 nm, d): 1 nm, e): 1 nm, and f): 100 nm.

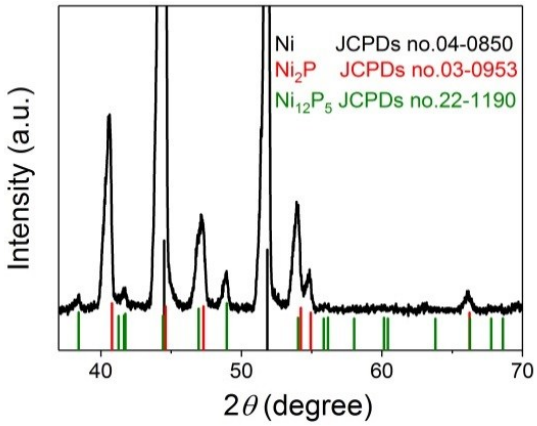

Fig. S16 XRD pattern of the Ni_xP-400/NF electrode after HER stability test.

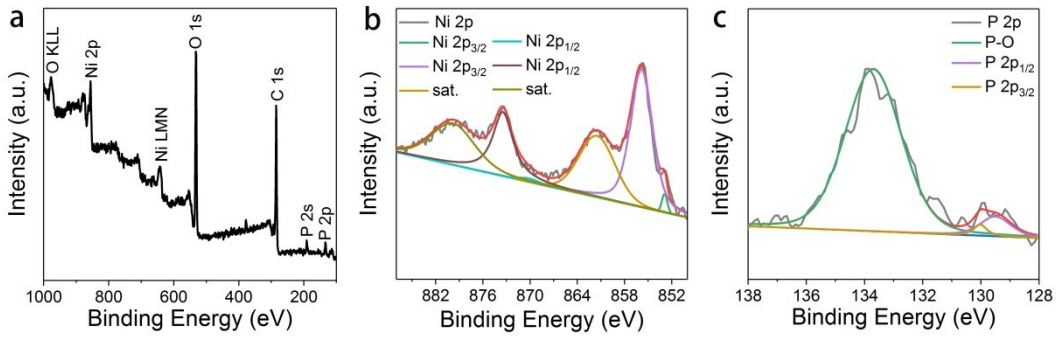

Fig. S17 XPS spectra of a) survey scan, b) Ni 2p, and c) P 2p for the Ni_xP-400 electrode after HER stability test.

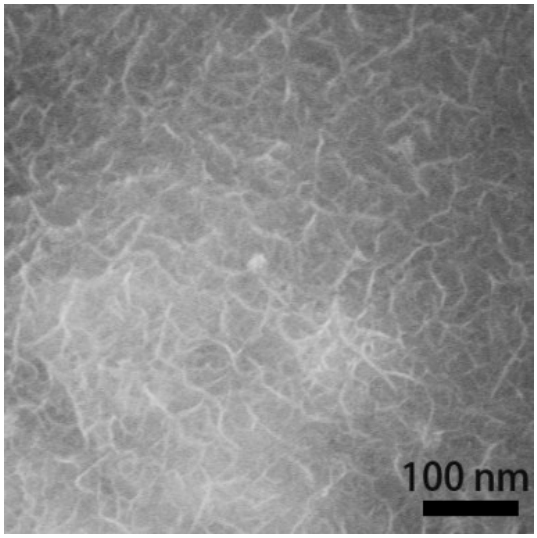

Fig. S18 SEM image of $FeNi(OH)_x$/NF.

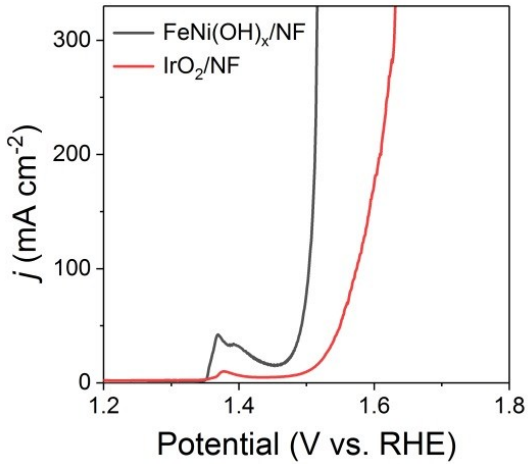

Figure S19. LSV curves of $FeNi(OH)_x$/NF and commercial IrO_2/NF.

Table S1. Comparison of HER activities of our self-supported tripod-like Ni_xP/NF NWs with recent reported metal phosphides catalysts in 1.0 M KOH.

Catalyst	j (mA cm^{-2})	η (mV)	Reference
Ni_xP-400	10 20 100	71 93 153	This work
NiP_2/NiO NRs	10	131	*ACS Appl. Mater. Interfaces*, 2018, **10**, 17896-17902
$Ni_{2(1-x)}Mo_{2x}P$	10 100	72 162	*Nano Energy*, 2018, **53**, 492-500
Co-P film	10 20 100	94 115 158	*Angew. Chem. Int. Ed.*, 2015, **54**, 6251-6254
CoP/NPC/TF	10	80	*Adv. Energy Mater.*, 2019, 1803970
$Ni_{12}P_5$/NF	10 20 100	170 209 290	*ACS Catal.*, 2017, **7**, 103-109
Ni_2P/NF	10 20 100	85 133 215	*ACS Catal.*, 2017, **7**, 103-109
Ni_2P/CNFs	10	108	J. Mater. Chem. A, 2019, **7**, 7451–7458
$NiMoP_2$ NW/CC	100	199	*J. Mater. Chem. A*, 2017, **5**, 7191-7199
Mo-Ni_2P/NF	10	78	*Nanoscale*, 2017, **9**, 16674-16679
Ni_2P/Fe_2P/NF	10	115	*J. Colloid Interface Sci.*, 2019, **541**, 279-286

$Ni_{0.51}Co_{0.49}P$	10	82	*Adv. Funct. Mater.*, 2016, **26**, 7644-7651

Table S2. Comparison of overall alkaline water splitting performance of our Ni_xP-400/NF||$FeNi(OH)_x$/NF couples with recent reported metal phosphides catalysts.

Catalyst	*j* (mA cm^{-2})	Potential (V)	Reference
Ni_xP-400/NF||$FeNi(OH)_x$/NF	10 100	1.53 1.62	This work
$Ni_5P_4@NiCo_2O_4$	100	1.65	*Adv. Energy Mater.*, 2018, **8**, 1801690
NiCoP/rGO||NiCoP/rGO	10	1.59	*Adv. Funct. Mater.*, 2016, **26**, 6785-6796
Ni_5P_4	10	Less than 1.7	*Angew. Chem. Int. Ed.*, 2015, **54**, 12361-12365
$Ni_{12}P_5$	10	1.64	*ACS Catal.*, 2017, **7**, 103-109
Ni_2P	10	1.58	*ACS Catal.*, 2017, **7**, 103-109
$NiMoP_2$||PE-$NiMoP_2$	10	1.67	*J. Mater. Chem. A*, 2017, **5**, 7191-7199
$Ni_{0.51}Co_{0.49}P$	10	1.57	*Adv. Funct. Mater.*, 2016, **26**, 7644-7651
$NiFeO_x$/NiFe-P	20 (onset)	1.6	*Adv. Energy Mater.*, 2017, **7**, 1700107
$Na_{0.08}Ni_{0.9}Fe_{0.1}O_2$ and NiP(-)	10	1.54	*Energy Environ. Sci.*, 2017, **10**, 121-128

S1. Y. Wang, Y. Sun, F. Yan, C. Zhu, P. Gao, X. Zhang and Y. Chen, *J. Mater. Chem. A.*, 2018, **6**, 8479-8487.

S2. W. Zhang, J. Qi, K. Q. Liu and R. Cao, *Adv. Energy Mater*., 2016, **6**, 1502489.

S3. F. Yan, C. Zhu, C. Li, S. Zhang, X. Zhang and Y. Chen, *Electrochim. Acta*, 2017, **245**, 770-779.